Available online at www.sciencedirect.com
ScienceDirect
International Journal of Thermal Sciences 47 (2008) 468–478
International Journal of Thermal Sciences
www.elsevier.com/locate/ijts

Design of a heat exchanger to reduce the exhaust temperature in a spark-ignition engine

Seokhwan Lee [a,1] Choongsik Bae [b,*],

[a] *Engine Research Center, Korea Institute of Machinery and Materials, 171, Jang-dong, Yuseong-gu, Daejeon, 305-343, Republic of Korea*
[b] *Department of Mechanical Engineering, Korea Advanced Institute of Science and Technology, 373-1, Guseong-dong, Yuseong-gu, Daejeon, 305-701, Republic of Korea*

Received 20 June 2006; received in revised form 12 March 2007; accepted 21 March 2007

Available online 10 May 2007

Abstract

A design of experiments (DOE) technique was used to design an exhaust heat exchanger to reduce the exhaust gas temperature under high load conditions in a spark-ignition engine. Through a limited number of experiments, the DOE evaluated the influence and the interaction of eight selected design parameters of the heat exchanger that affect the cooling performance of the exhaust gas. The heat exchanger was installed between the exhaust manifold and the inlet of the close-coupled catalytic converter (CCC) to avoid thermal aging. To maximize the heat transfer between the exhaust gas and coolant, fins were implemented at the inner surface of the heat exchanger. The design parameters consisted of the fin geometry (i.e., length, thickness, arrangement, and number of fins), coolant direction, exchanger wall thickness, and the length of the heat exchanger. The DOE results were analyzed and the acceptable range of each design parameter is discussed.

Keywords: Design of experiment (DOE); Heat exchanger; Close-coupled; Catalytic converter (CCC); Thermal aging; Heat transfer

1. Introduction

Due to an increase in environmental regulations such as EURO-IV and Ultra Low Emission Vehicle (ULEV) emission standards, a great deal of attention has been directed towards environmental hazards and energy conservation. Reduction of exhaust emissions from spark-ignition (SI) engines is usually accomplished with the use of catalysts [1]. At high engine loads, the exhaust gas temperature is greatly increased, which could result in accelerated aging of the catalyst coating [2]. After the adoption by most automotive manufacturers of Pd-containing close-coupled catalyst systems to meet stringent concurrent emission standards, higher thermal loads exerted on the converter system during the high load condition become more serious [3,4]. The catalyst could suffer from a significant reduction in Brunauer Emett Teller (BET) surface area or, in some cases, a catastrophic substrate melt down due to the high catalyst temperature [5]. In order to reduce the exhaust gas temperature without loss of power, additional fuel is usually injected to formulate a richer mixture. However, this approach not only wastes fuel, but it also increases the emission of carbon monoxide (CO) and hydrocarbon (HC).

In this study, the exhaust gas temperature was reduced during high load conditions by using a small water-cooled heat exchanger, which, in principle, acts like an exhaust gas recirculation (EGR) cooler [6]. As shown in Fig. 1, this heat exchanger was installed between the exhaust manifold and the inlet of the close-coupled catalytic converter to transfer the exhaust thermal load from the exhaust gases to the engine coolant. To maximize the convective effect between the exhaust gas and coolant, fins were utilized at the inner surface of the heat exchanger [7]. This heat exchanger was very easy to install and inexpensive to manufacture. In addition, it provided an alternative way to reduce the exhaust gas temperature at a higher engine load without wasting fuel. However, care must be taken such that there is not an increase in the engine back-pressure and the catalyst light-off time [8].

* Corresponding author. Tel.: +82 42 869 3044; fax: +82 42 869 5044.
E-mail addresses: shlee@kimm.re.kr (S. Lee), csbae@kaist.ac.kr (C. Bae).
[1] Tel.: +82 42 868 7420; fax: +82 42 868 7305.

1290-0729/$ – see front matter
doi:10.1016/j.ijthermalsci.2007.03.011

Nomenclature

CCC	Close-Coupled Catalyst		
C_{pg}	Gas specific heat	J/kg K	
D_h	Hydraulic diameter	m	
h_h	Heat transfer coefficient	W/m^2 K	
k_f	Thermal conductivity of the fin	W/m K	
k_e	Thermal conductivity of the exhaust gas	W/m K	
$\dot{m}_{air}$	Intake air mass rate	kg/s	
$\dot{m}_{fuel}$	Fuel mass rate	kg/s	
$\dot{M}_g$	Exhaust gas mass rate	kg/s	
N	Fin number		
Nu	Nusselt number		
$\dot{Q}$	Heat exchange rate	W	
q_t	Total rate of heat transfer from the fins and unfinned surface	W	
S/N	Signal to noise ratio		
S_T	Total sum of squares		
T_b	Fin base temperature	K	
T_e	Exhaust gas temperature	K	
T_{cat_ref}	Gas temperature at the catalyst without a heat exchanger	K	
T_{cat_sam}	Gas temperature at the catalyst with each sample of heat exchanger	K	
V_e	Variance		
β	Index of cooling performance		
ε_f	Fin effectiveness		
η_f	Fin efficiency		
η_o	Total surface efficiency		
λ	Lambda value		
θ_b	Difference in temperature between the fin base and the exhaust gas	K	

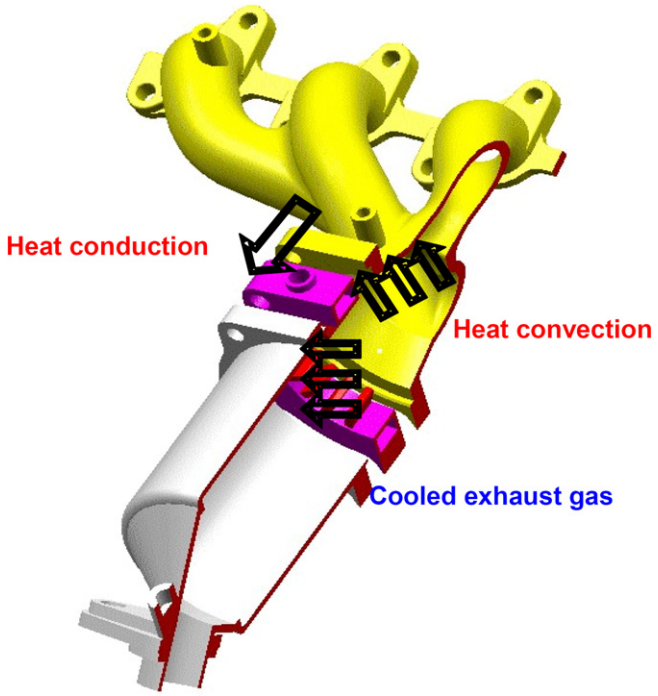

Fig. 1. Schematic diagram of the heat exchange phenomena between the exhaust system and heat exchanger.

The DOE (design of experiments) approach was applied to limit the number of experiments needed to define the effects of the geometric design parameters (i.e., fin length, thickness, arrangement, and number of fins) [9]. This technique is widely used to design an optimized product or process. DOE is very useful to optimize the machine tool process like extrusion [10], the operating conditions for a small engine [11], and the machine component such as gas turbine [12].

In this study, it was found that testing eighteen heat exchangers with different geometries was enough to identify the optimal design parameters using the DOE. An engine test was performed on the eighteen heat exchangers and the heat flux was calculated under different conditions. Statistical analysis was performed to identify the optimum design with consideration of the operating conditions.

2. Design of experiments (DOE)—optimization process of designing a heat exchanger

Design of experiments (DOE) is a scientific approach that allows the experimenter to understand a process and to determine how the input variables (i.e., factors) affect the output or quality characteristics [13]. The conventional approach to testing is to change the input variables in a serial fashion and then evaluate the effects of the changes on the system outputs. In contrast, DOE deals with simultaneous changes to more than one system variable by designing a matrix of test points after the variables have been chosen. Since a single matrix test point can involve several variables being changed at once, the interactions between variables can be quantified in addition to the singular effects of individual variables on the system responses [14]. To apply the DOE technique on the heat exchanger using the Taguchi method [8,15], signal, noise and control factors had to be identified. These factors are represented by the P-diagram shown in Fig. 2, which expresses the functional requirements and the relationship between these three categories of factors: output response, side effects, and failure modes. A summary of the factors included in each category is presented hereinafter.

2.1. Signal factors

Signal factors are set by the user or operator to achieve the target performance [14]. In this study, engine load was used as a signal factor and the heat flux rate was used as an output response. When the engine was operated at higher loads, the fuel supply (i.e., chemical energy) to the engine increased, resulting in a higher output of thermal energy. Subsequently, the heat transfer from exhaust gas to heat exchanger increased. Fig. 3 assumes a linear relationship between the signal factor and output

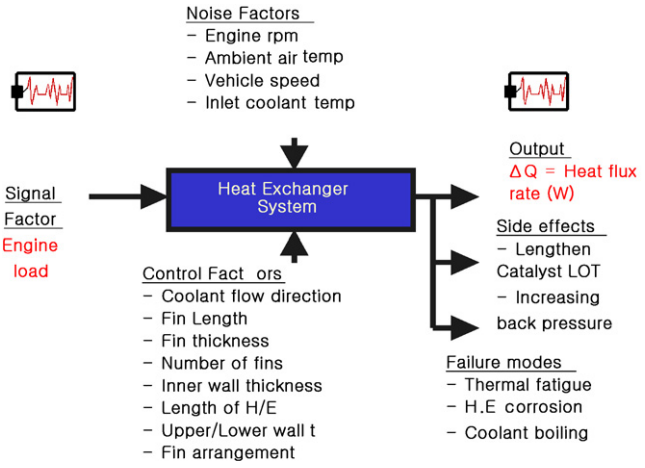

Fig. 2. Parameter diagram (P-diagram) for the cooling system.

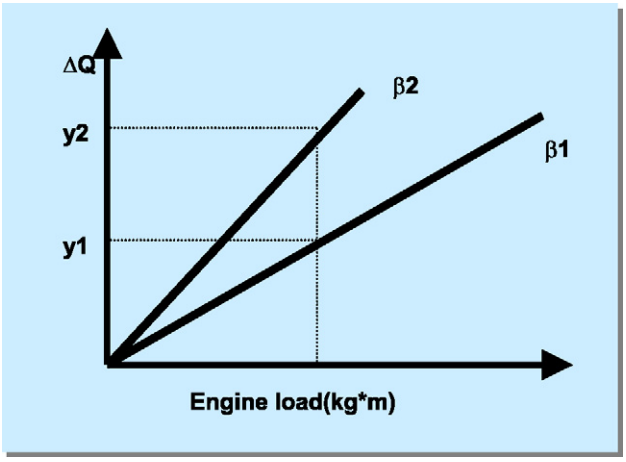

Fig. 3. The linear relationship between the signal factor and output response.

Table 1
Signal factors

Signal Factor	M 1	M 2	M 3	M 4	M 5
Relative Load	20%	30%	40%	50%	60%

response. This line was determined by fitting the experimental points using the least square method. The slope of this diagonal line, referred to as sensitivity, is denoted by β. When the slope β is steeper, the cooling performance of the heat exchanger increased. Table 1 expresses the signal values for different relative engine loads, M_1 through M_6, used in this study. Relative load means the percentage of the ratio of current load to full load based on engine torque, i.e., at 2000 rpm; the full load is 74 N m and at 450 rpm; full load is 82 N m for this engine.

2.2. Noise factors

During actual production conditions, noise factors are difficult, expensive, and hard to control; however, they may be controllable during experimentations [14]. These factors cause the performance characteristics of a product to deviate from its target or nominal value. The noise factors that could affect the heat exchanger performance are engine rpm, ambient temperature, vehicle speed, and inlet coolant temperature. If all the noise factors are individually taken into account, the experiments have to be conducted for two values of each noise factor. However, only two representative values were used since the objective of the DOE is not to consider the contribution of each noise factor. This system uses the engine water pump as a power source of coolant circulation so that an increase in engine speed increases the coolant circulation rate. Therefore, a low engine speed at $N_1 = 2000$ rpm and a high engine speed at $N_2 = 4500$ rpm could represent the noise factors at each signal (i.e., engine load). A higher vehicle speed is beneficial in cooling down the heat exchanger. To simulate the ambient temperature and vehicle speed at each noise factor condition, a cooling fan was introduced for the experiments at a higher engine speed, while a small heater was switched on during the low engine speed test. Table 2 expresses the noise factors.

Table 2
Noise factors

Noise	Condition	Engine Speed	Engine room temp	Vehicle speed
N1	Low ΔQ	2000 rpm	90°C	0 km/h
N2	High ΔQ	4500 rpm	50°C	130 km/h

2.3. Control factors

Control factors or design parameters are those factors that can be controlled easily during actual production conditions or standard conditions. It was the objective of the design activity to determine the optimum value of these factors to achieve product or process robustness. Eight parameters related to heat exchanger design were selected, considering major geometric parameters affecting heat transfer [6,7], as control factors as shown in Fig. 4: coolant flow direction (A), fin length (B), fin thickness (C), number of fins (D), inner wall thickness (E), length of heat exchanger (F), upper/lower wall thickness (G), and fin arrangement (H). As shown in Table 3, three levels for each factor were selected, except factor A, which had only two levels, so that a better optimization of the design could be acquired. Factors A and H were chosen to take into account the non-symmetry of the four branch pipes of the exhaust manifold used in this study. The unsymmetrical shape causes an uneven temperature profile, which was highest at the right side of the catalyst substrate [16]. Fig. 5 shows the simulation results of this heat distribution obtained by a commercial simulation program.

2.4. Orthogonal array experiments

The main benefits of the DOE include significant reductions in the number of initial tests required ($2 \times 3^7 = 4374$), quantification of interactions between variables, and prediction of system responses to variable settings. This study selected eight control factors, where one factor had 2 levels and the others had 3 levels. According to the DOE method, the L_{18} orthogonal array (OA) can handle one factor at two levels and seven factors at

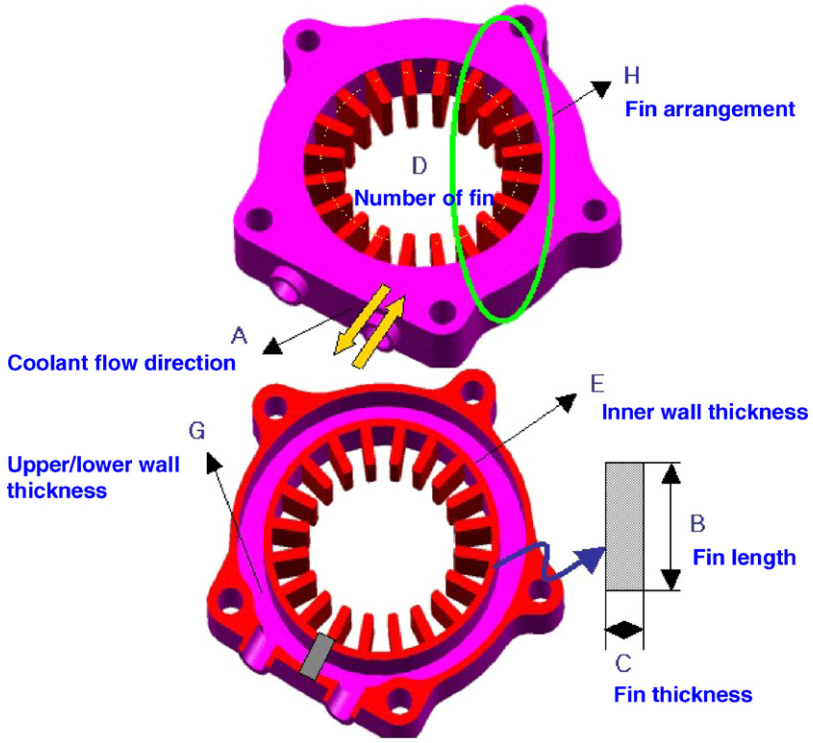

Fig. 4. The schematic diagram of control factors.

Table 3
Control factors

	Control Factor	Level1	Level2	Level3
A	Coolant flow direction	Clockwise	Counter clockwise	-
B	Fin length	10 mm	15 mm	20 mm
C	Fin thickness	1.5 mm	2 mm	2.5 mm
D	Number of fins	10	15	20
E	Inner wall thickness	2 mm	3 mm	4 mm
F	Length of Heat exchanger	18 mm	20 mm	22 mm
G	Upper/Lower wall thickness	3 mm	4 mm	5 mm
H	Fin arrangement	1:1	1:1.3	1:1.6

three levels. The ability to handle three-level factors makes the L_{18} ideal for studying the control factors in optimization. The levels of factors assigned for the eighteen-run OA are listed in Table 4. The OA is a method of setting up experiments that only require a fraction of the full factorial combinations. The treatment combinations are chosen to provide sufficient information to determine the factor effects using the analysis of means. The OA imposes an order on the way the experiment is carried out. OA refers to the balance of the various combinations of factors so that no one factor is given more or less weight in the experiment. Additionally, OA refers to the fact that the effect of each factor can be mathematically assessed independently of other factor effects [14].

An OA is a matrix of numbers arranged in rows and columns. Each row represents the level (or states) of the selected factors in a given experiment, while each column represents a specific

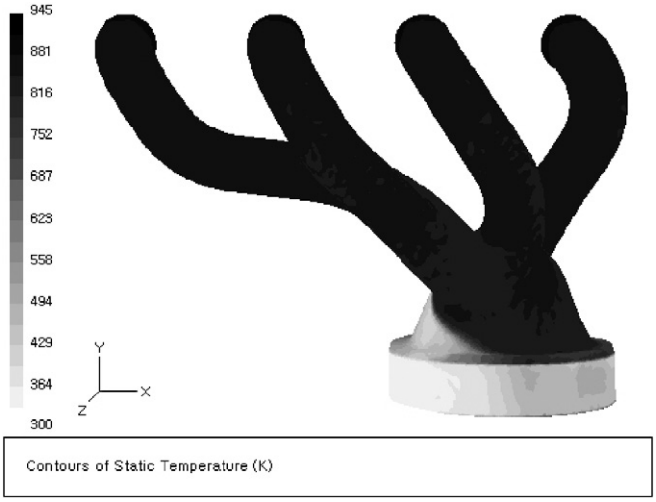

Fig. 5. Simulation results of the heat distribution.

factor whose effects on the output (or response) are of interest to the experimenters. In the blank, the heat flux rate, which was selected as an output response, had to be filled out at each experimental condition. Therefore, 18 samples were built and the response $y =$ heat transfer rate was measured. Fig. 6 shows photographs of the 18 samples.

3. Experimental setup and operating conditions

As mentioned above, 18 heat exchangers with different geometries (i.e., levels) were individually tested in a test bed with a 1.0L SI engine at five engine loads and two engine speeds for each load.

Table 4
L_{18} orthogonal array to find the optimal level of each control factor

SAMPLES	A	B	C	D	E	F	G	H	M : 20%		M : 30%		M : 40%		M : 50%		M : 60%	
									N1	N2	N1	N2	N1	N2	N1	N2	N1	N2
1	1	1	1	1	1	1	1	1										
2	1	1	2	2	2	2	2	2										
3	1	1	3	3	3	3	3	3										
4	1	2	1	1	2	2	3	3										
5	1	2	2	2	3	3	1	1										
6	1	2	3	3	1	1	2	2										
7	1	3	1	2	1	3	2	3										
8	1	3	2	3	2	1	3	1										
9	1	3	3	1	3	2	1	2										
10	2	1	1	3	3	2	2	1										
11	2	1	2	1	1	3	3	2										
12	2	1	3	2	2	1	1	3										
13	2	2	1	2	3	1	3	2										
14	2	2	2	3	1	2	1	3										
15	2	2	3	1	2	3	2	1										
16	2	3	1	3	2	3	1	2										
17	2	3	2	1	3	1	2	3										
18	2	3	3	2	1	2	3	1										

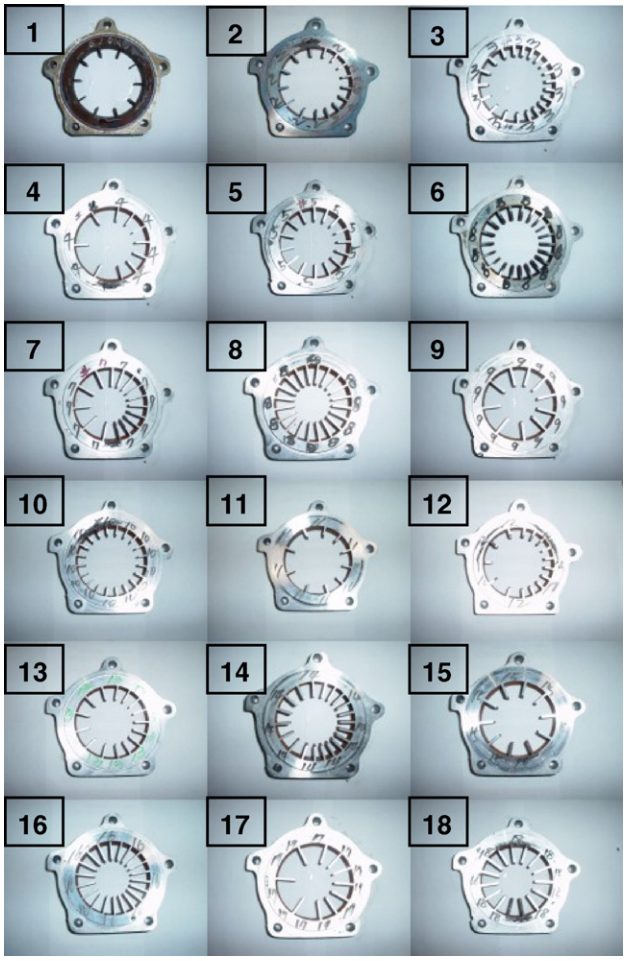

Fig. 6. Photographs of the 18 samples used to find the optimal level of each control factor.

3.1. Test engine

The engine was fitted with a programmable electronic control unit (ECU) as shown in Fig. 7. The engine was equipped with a close-coupled catalyst (CCC) and under-floor catalytic converter (UCC) to meet the Euro-III emission legislation. The tests were conducted with the engine coupled to an eddy-current dynamometer (maximum brake power = 176 Ps/3200 rpm, maximum brake torque = 39.0 kg m). To monitor the engine operating parameters (such as relative load, mass of intake air, coolant temperature, and lambda value) and to change the fuel mapping data, both a programmable Engine Management System, NTK (EMS) and a data acquisition system (ETAS MAC2) were used. Thermocouples and thermoscan were installed to thermally monitor the exhaust system. A wide-band O_2 sensor and a lambda meter were also employed to control the air/fuel ratio of the engine. A summary of the engine features is shown in Table 5. The water pump inside of the engine was used to circulate the coolant to the heat exchanger. This study used a mixture of 50% water and 50% ethylene glycol as a coolant. Fig. 7 also shows a scheme of the coolant circulation between the engine and heat exchanger. The coolant running to the heat core was a source of the coolant through the heat exchanger and the coolant supply increased with the engine speed due to the water pump. The water pump was directly connected to the engine and the work of the pump increased with engine speed.

3.2. Temperature measurement

K-type thermocouples were used to monitor exhaust gas temperature before the catalyst, the catalyst temperature, and the coolant temperatures at the inlet and outlet of each heat exchanger. To measure the temperature of the catalyst, thermocouples were installed 50 mm from the front face of the catalyst bed along the central axis, which is 40 mm from the upper face. It was assumed that this mid-position was the most active in the catalytic reaction. The temperatures were measured at 2000 and 4500 rpm under various engine loads after reaching the steady state values.

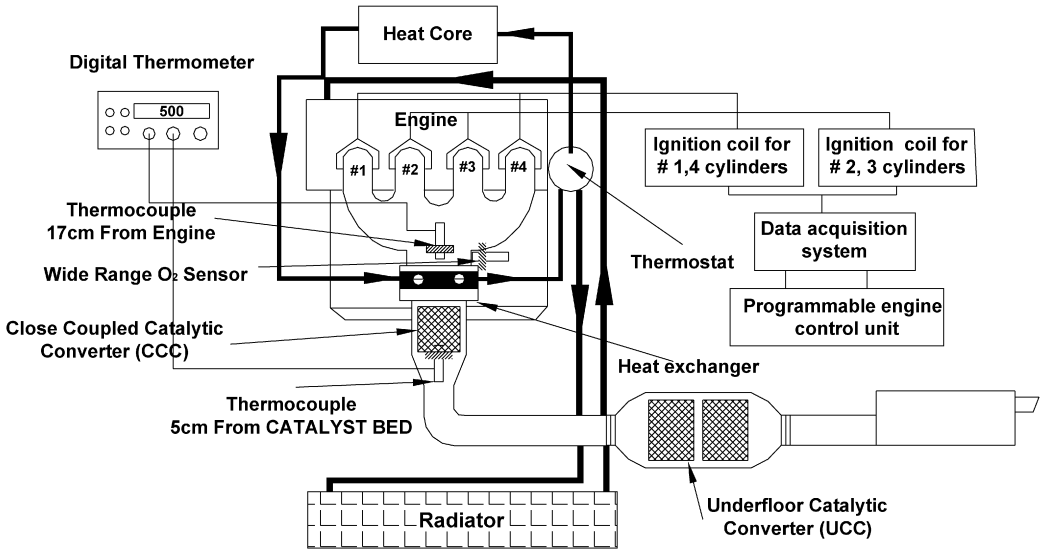

Fig. 7. Engine test facility and coolant circulation scheme.

Table 5
Engine specifications

Specifications	Resources
Cylinder	4
Bore (mm)	66
Stroke (mm)	73
Bore pitch (mm)	72.5
Displacement (cc)	999
Compression ratio	9.8

4. Fin effectiveness and heat flux calculation

4.1. Fin effectiveness

To maximize the convective effect between the exhaust gas and coolant, fins were utilized at the inner surface of the heat exchanger. The geometries of fins are the most important factors in heat exchanger optimization. A simple fin model was introduced to emphasize the great role of fins to improve the heat exchanger performance and estimate the heat exchanger performance.

There is no assurance that the heat transfer rate will be increased through the use of fins because the fin itself represents a conduction resistance. An assessment of this matter may be made by evaluating the fin effectiveness ε_f. It is defined as the ratio of the fin heat transfer rate to the heat transfer rate that would exist without fin. Another measure of fin thermal performance is provided by the fin efficiency η_f. The maximum rate at which a fin could dissipate energy is the rate that would exist if the entire fin surface were at the base temperature [17].

Fig. 8 shows a wall with a fin on the exhaust gas side. Heat transfer took place from the fin surface, as well as the unfinned surface. The fin was assumed to have an efficiency (η_f), fin number (N), surface fin area (A_f), and total area (A_t), which was the area associated with A_f and exposed area A_b.

The total rate of heat transfer by convection from the fin and the unfinned surface, q_t, may be expressed as

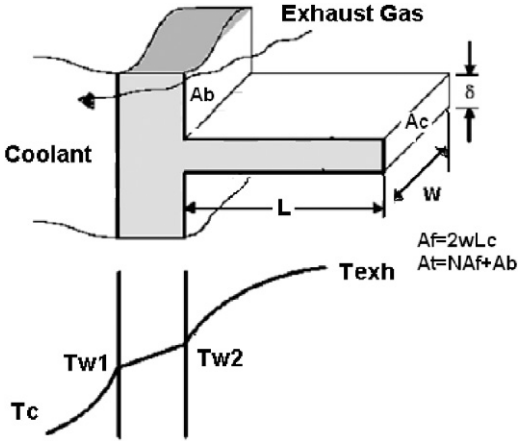

Fig. 8. Heat flow through the wall of a finned flat tube.

$$q_t = N\eta_f h A_f \theta_b + h A_b \theta_b,$$
$$\theta_b = T_e - T_b = h\left[N\eta_f A_f + (A_t - NA_f)\right]\theta_b$$
$$= hA_t\left[1 - \frac{NA_f}{A_t}(1-\eta_f)\right]\theta_b \quad (1)$$

Where the convection coefficient h is assumed to be equivalent for the finned and prime surface and η_f is the efficiency of a single fin. θ_b is the difference in temperatures between the fin base, T_b, and the exhaust gas, T_e.

$$A_t = NA_f + A_b, \quad A_f = 2wL_c, \quad L_c = L + \frac{\delta}{2} \quad (2)$$

(w: width, δ: thickness, L: length of the fin).

The fin efficiency (η_f) was calculated as follows for a flat tube heat exchanger as a function of its cross-section area A_c, length L_c, thermal conductivity of the fin k_f and heat transfer coefficients (k_f, h) [17].

$$\eta_f = \frac{\tanh mL_c}{mL_c} \quad (3)$$

If the heat exchanger has rectangular fins, the perimeter may be approximated as $P = \pi D + 2NL_c$, and

$$mL_c = \left(\frac{hP}{k_f A_c}\right)^{1/2} = \left(\frac{2h}{k_f \delta}\right)^{1/2} L_c \tag{4}$$

$$m = \sqrt{\frac{2h}{k_f \delta}} \tag{5}$$

A number of forced convection heat transfer correlations have been developed for laminar and transitional turbulent flows [6]. In this study, the heat transfer coefficient on the coolant-side of the heat exchanger h_h was given by Eq. (6).

$$h_h = Nu \cdot \frac{k_e}{D_h} \tag{6}$$

Where Nu is the Nusselt number and has been calculated by (see detail in Ref. [6]):

$$Nu = \frac{\text{Fluid layer resistance}}{\text{Convective resistance}} = \frac{(x/k_e)}{(1/h)} = 0.33581\, Pr^{0.33} Re^{0.52376} \tag{7}$$

The value of the Nusselt number is varied with engine operating conditions (speed and load) and each heat exchanger between 11 and 33.

It was assumed that the convective heat transfer coefficient along the fin was constant though it may vary. This simplification is supposed to be still valid for the general optimization process.

For flow through a tube, the characteristic length x, is defined as the hydraulic diameter, D_h.

$$D_h = \frac{4 \times \text{Flow area}}{\text{Wetted parameter}} = \frac{4A}{P} = \frac{4(\frac{\pi}{4}D^2 - NL_c\delta)}{\pi D + 2NL_c} \tag{8}$$

The fin effectiveness (the ratio of the fin heat transfer rate to the heat transfer rate without the fin) may be expressed as:

$$\varepsilon_f = \frac{q_t}{hA_b\theta_b} = \left[1 - \frac{NA_f}{A_t}(1 - \eta_f)\right] \times \frac{A_t}{\pi D w} \tag{9}$$

4.2. Heat flux

In order to calculate the heat flux transferred from the exhaust gas due to the heat exchanger, the catalyst temperature reduction was measured for each of the 18 samples. The heat flux rate was then determined according to the following equation:

$$\dot{Q} = \dot{M}_g \times C_{pg} \times \left(T_{\text{cat\_ref}} - T_{\text{cat\_sam}}\right) \tag{10}$$

Where, $\dot{M}_g$ is the exhaust gas mass rate, C_{pg} is the gas specific heat, $T_{\text{cat\_ref}}$ is the gas temperature at the catalyst without a heat exchanger (BASE), and $T_{\text{cat\_sam}}$ is the gas temperature at the catalyst with each sample of the heat exchanger (H/E).

$\dot{M}_g$ was estimated from measuring the air mass rate from the ECU data and by assuming the engine was operated at stoichiometric conditions. Accordingly, the exhaust gas mass rate could be calculated as follows:

$$\dot{M}_g = \dot{m}_{\text{air}} + \dot{m}_{\text{fuel}} = \left(1 + \frac{1}{14.6}\right) \times \dot{m}_{\text{air}} \quad (\text{for } \lambda = 1.0 \text{ condition}) \tag{11}$$

Where, $\dot{m}_{\text{air}}$ is the intake air mass rate and $\dot{m}_{\text{fuel}}$ is the fuel mass rate.

5. Analysis of variance (ANOVA)

Analysis of variance (ANOVA) is a computational technique that enables the engineer to quantitatively estimate the relative contribution of each control factor in the overall output response and express it as a percentage. ANOVA uses a mathematical technique known as the sum of squares to quantitatively examine the variation between the control factors from the overall experimental mean response [14]. Using ANOVA, the following calculations were performed to get the signal to noise factor and its slope.

(1) To calculate the sum of squares of the signal factor levels r and to define r_0:

$$r = M_1^2 + M_2^2 + M_3^2 + M_4^2 + M_5^2, \tag{12}$$

where r_0 is the number of the heat transfer data points obtained at each noise level, which, in this case, was equal to 2. These two values were obtained to take into account the effect on noise factors.

(2) To calculate the total sum of squares of the output signal for each set of data:

$$S_T = \sum_{i=1}^{n} y_i^2 = y_1^2 + y_2^2 + \cdots + y_n^2 \tag{13}$$

where y_i is the individually observed heat transfer rate at each input signal and each noise factor and n is the number of data points in the outer array (= 10). S_T (the total sum of squares) was then decomposed into S_e and S_β as follows:

$$S_T = S_e + S_\beta \tag{14}$$

where

$$S_\beta = \frac{1}{r_0 \times r}(M_1Y_1 + M_2Y_2 + M_3Y_3 + M_4Y_4 + M_5Y_5)^2. \tag{15}$$

Here, Y_i is the sum of the individually observed response value at each signal factor ($Y_1 = y_1 + y_2$).

(3) To calculate the variance V_e and signal to noise ratio (S/N ratio):

$$V_e = \frac{S_e}{n-1} \tag{16}$$

$$S/N = \eta_{\text{dB}} = 10 \times \text{Log}\frac{\frac{1}{r \times r_0}(S_\beta - V_e)}{V_e} \tag{17}$$

(4) To calculate the cooling performance β, the experimental points were fitted by a line passing through the zero point using the least square method. The slope of the line was identified as follows:

$$\sum_{i=1}^{m}\sum_{j=1}^{r_0}(y_{ij}-\beta M_i)M_i = 0$$

$$\beta = \frac{\sum_{i=1}^{m}\sum_{j=1}^{r_0} y_{ij}M_i}{\sum_{i=1}^{m}\sum_{j=1}^{r_o}(M_i)^2} = \frac{(M_1Y_1 + M_2Y_2 + M_3Y_3 + M_4Y_4)}{r_0 \times (M_1^2 + M_2^2 + M_3^2 + M_4^2)} = \frac{1}{r_0 \times r}(M_1Y_1 + M_2Y_2 + M_3Y_3 + M_4Y_4) \quad (18)$$

6. Results and discussion

6.1. Heat flux and fin effectiveness of each heat exchanger

Since the objective of this work was to maximize the heat transfer in the heat exchanger at higher engine loads, the optimum design became the one that achieved more heat transfer at higher engine loads. The heat flux versus the engine loads for each heat exchanger at 2000 and 4500 rpm was plotted as shown in Fig. 9. In these graphs, the experimental points could be approximately fitted with a line forced to the zero point using the least square method. The slope of the line represented the cooling performance β, which was estimated for each heat exchanger. Fig. 9 shows that sample 18 had maximum cooling performance ($\beta = 6203.2$), while sample 1 had the minimum value ($\beta = 2831.2$). However, sample 18 did not have the maximum fin effectiveness of the heat exchangers. Fig. 10 shows that sample 8 and 16 gave the largest fin effectiveness, whereas samples 1 and 11 gave the smallest. These results show that, for this application, the highly effective heat exchanger did not necessarily have the maximum fin effectiveness. This was attributed to the fact that the ratio of the heat transfer to the engine power was the factor needing to be maximized. Although sample 18 showed the greatest fin effectiveness, it was not the optimum design. The next section includes the necessary analysis to obtain the optimum geometrical parameters.

6.2. Analysis of variance to obtain the optimum geometrical parameters

From the analysis of variance, the calculated performance value β and S/N ratio could be acquired. The S/N ratio reflects the variability in the response of a system caused by noise factors. The average value of β was about 4783.2 and as expected from Fig. 9, sample 18 showed the best performance while sample 1 showed the worst. Table 6 shows the relative contribution of each level of control factors to the β value and S/N ratio. Fig. 11 displays the response graph of the S/N ratio and β value. In the case of the S/N ratio, there was only a slight variation for each level of the control factors. The results demonstrated that the noise factor had hardly any affect on the performance of the heat exchanger. Hence, it was important to consider the β value to find the optimal level of control factors. The optimal levels of each control factor were A_2, B_3, C_3, D_3, E_2, F_2, G_2, and H_3. In the case of the A, B, C and D factors, the variation of the β value was greater than those of E, F, G, and H. These results showed that the fin geometric parameters (i.e., length, thickness, and number) and the direction of the circulating coolant were the main factors affecting the cooling performance of the heat exchanger.

6.3. Confirmation test

Having identified the optimal level of each control factor, the optimum heat exchanger was manufactured and tested. Fig. 12 shows a photograph of the optimal heat exchanger. The purpose of the confirmation test was to ensure that S/N ratio and β value of the optimized sample could be reproduced under realistic operating conditions. If the S/N ratio and β value of the confirmation test is close to those of the optimized sample, it can be concluded that the functional robustness and sensitivity of the optimized sample are reproduced under realistic operating conditions [18–20].

Confirmation tests also check the results of the parameter optimization experiment, demonstrate the optimum performance, and confirm freedom from interaction. An interaction between two control factors means that the dependence of one experimental factor on the level of another experimental factor for its contribution to the measured response. Significant interactions cause the response to deviate from the value predicted by DOE process. When confirmation tests fail, this is one of the probable cause. When the S/N ratio behavior matches the prediction, including only the main effects and no interaction terms, then the design is free of interactions [14].

The analysis of mean (ANOM) is achieved by taking averages of the β values that correspond with the factor level to estimate each factor effect's contribution [14]. The predicted cooling performance (β) of the optimal sample A_2, B_3, C_3, D_3, E_2, F_2, G_2, H_3 according to the ANOM was:

$$\beta_{\text{opt}} = \overline{T} + (\overline{T}_{A_2} - \overline{T}) + (\overline{T}_{B_3} - \overline{T}) + (\overline{T}_{C_3} - \overline{T}) + (\overline{T}_{D_3} - \overline{T}) + (\overline{T}_{E_2} - \overline{T}) + (\overline{T}_{F_2} - \overline{T}) + (\overline{T}_{G_2} - \overline{T}) + (\overline{T}_{H_3} - \overline{T}) = 6721.6 \quad (19)$$

where $\overline{T}$ is the overall average response of β for the entire orthogonal array and $\overline{T}_{A_2}$, $\overline{T}_{B_3}$, $\overline{T}_{C_3}$, $\overline{T}_{D_3}$, $\overline{T}_{E_2}$, $\overline{T}_{F_2}$, $\overline{T}_{G_2}$, $\overline{T}_{H_3}$ are the response averages for factors A_2, B_3, C_3, D_3, E_2, F_2, G_2 and H_3, respectively.

The β value of confirmation acquired after conducting experiments on the optimum heat exchanger was found to be 6576.3, which was 2% less than the predicted value due to manufacturing tolerances and measurement errors. Compared with the initial design (sample 1), the optimal sample showed that the cooling performance more than doubled. The predicted gain in the S/N ratio between the initial design and the optimal design was 0.23 dB. Table 7 illustrates the predicted and confirmed S/N ratio and β value of the optimal and initial designs. Additionally, this table shows that the gain in the S/N ratio and β value were reproducible. This confirms the functional robustness of the optimized sample along the operating conditions and the independence of the control factors.

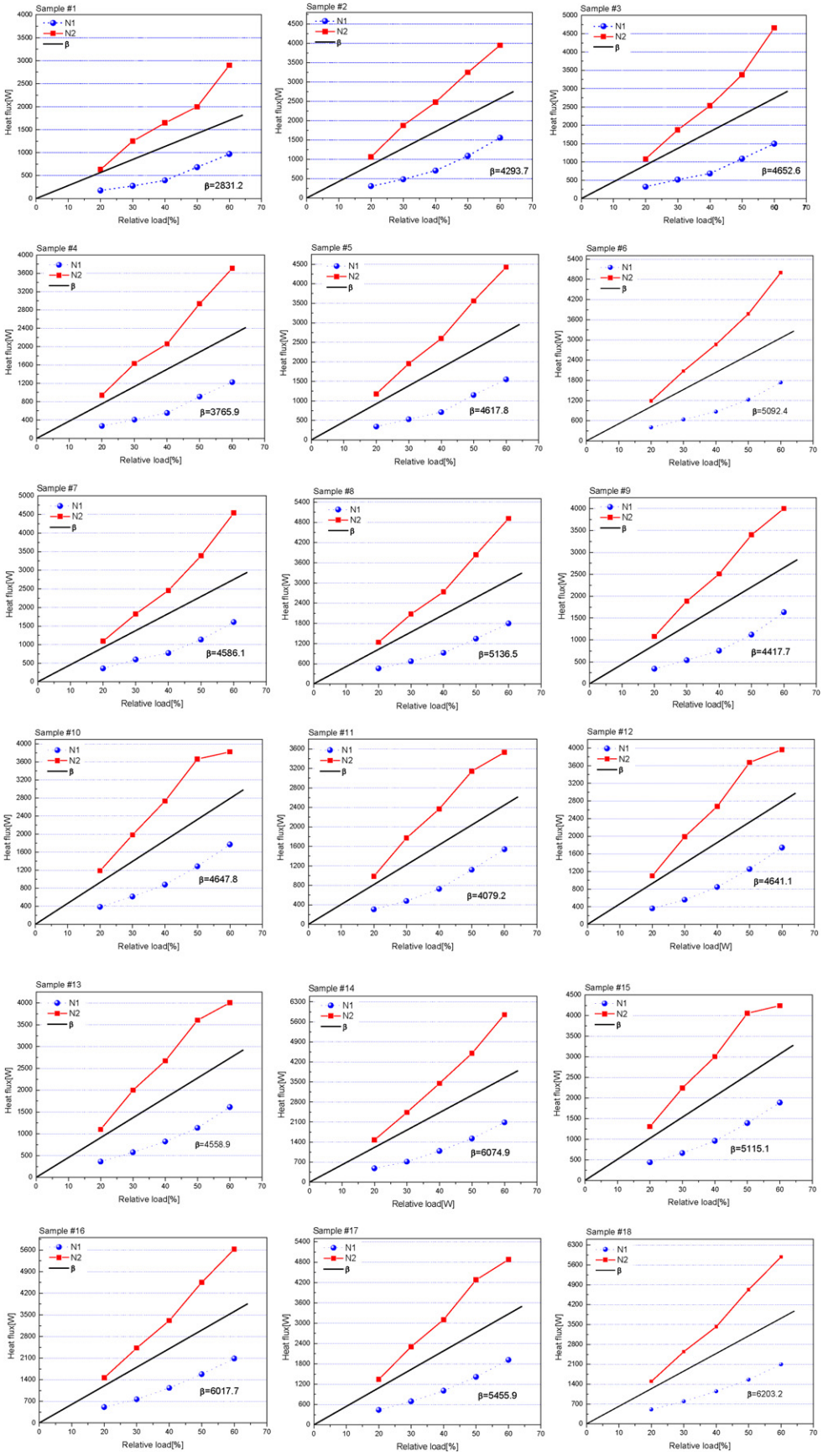

Fig. 9. Heat flux of the representative 18 samples at 2000 rpm (N1 condition) and 4500 rpm (N2 condition).

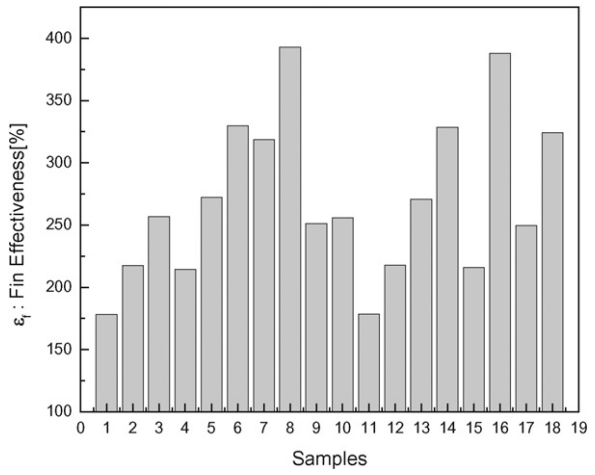

Fig. 10. The theoretical fin effectiveness of the heat exchangers (samples 1–18).

Table 6
Relative contribution of each level of the control factors to the S/N ratio

Factor	S/N	β	Factor	S/N	β
A1	12.616	4367.1	E1	12.792	4811.15
A2	13.262	5199.3	E2	13.067	4828.34
			E3	12.957	4710.1
B1	12.979	4175.9	F1	12.916	4619.34
B2	12.79	4870.8	F2	12.962	4900.53
B3	13.047	5302.8	F3	12.938	4829.72
C1	12.835	4401.3	G1	12.865	4766.72
C2	13.008	4943	G2	13.135	4865.16
C3	12.974	5005.3	G3	12.816	4717.71
D1	12.93	4277.5	H1	12.987	4758.58
D2	12.94	4816.8	H2	13.068	4743.26
D3	12.946	5255.3	H3	12.762	4847.74

7. Conclusions

Design of experiment (DOE) was used to investigate the effect of geometrical parameters of 18 heat exchangers to clarify the effect of the fin shape to the heat exchanger cooling efficiency. From the engine tests with an optimal sample, which was acquired from DOE results, the following conclusions were obtained:

1. The DOE analysis showed that the fin geometric parameters (i.e., length, thickness, and number) and the direction of the circulating coolant were the main factors affecting the cooling performance of the heat exchanger.
2. The heat exchanger that has maximum effectiveness was not necessarily the optimum design.
3. In comparison with the initial design (sample 1), the optimal sample showed that the cooling performance more than doubled.

Table 7
The predicted and confirmation test values for the S/N ratio and β

	Predicted		Confirmation test	
	S/N	β	S/N	β
Initial design	12.32	2696	12.09	2831.2
Optimal design	13.62	6721.6	13.02	6576.3
Gain	0.70dB	149%	0.93dB	157%

4. The predicted gain in the S/N ratio between the initial design and the optimal design was 0.23 dB.
5. The gain in the S/N ratio and β value were reproducible, which confirmed the functional robustness of the optimized sample along the operating conditions.

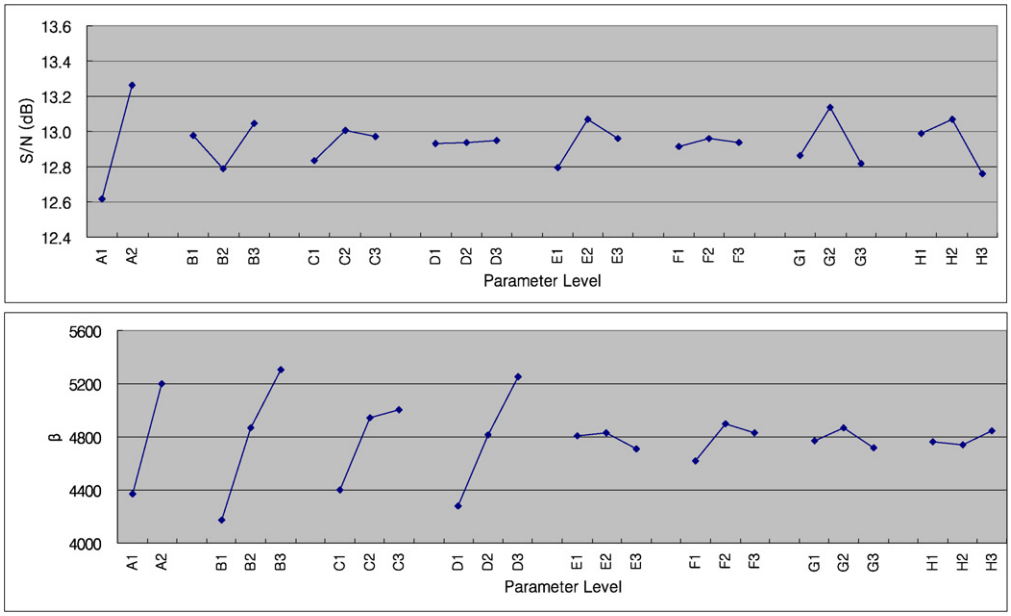

Fig. 11. Response graph of the S/N ratio and β.

Fig. 12. A photograph of the optimal heat exchanger.

Acknowledgements

The authors would like to acknowledge the financial and technical support of Basic Research Fund in KIMM and Combustion Engineering Research Center (CERC) in KAIST. The authors appreciate the technical support of Mr. Taesik Han, Mr. Jongik Jeon, and Dr. Yongpyo Lee.

References

[1] M.E. Crane, R.H. Thring, D.J. Podnar, L.G. Dodge, Reduced cold-start emissions using Rapid Exhaust Port Oxidation (REPO) in a spark engine, SAE 970264, 1997.
[2] Y.K. Lui, J.C. Dettling, Evolution of Pd/Rh TWC catalyst technology, SAE930249, 1993.
[3] R.J. Brisley, R.D. O'Sullivan, A.J.J. Willkins, The effect of high temperature ageing on platinum–rhodium and palladium–rhodium three way catalysts, SAE 910175, 1991.
[4] T. Nagel, W. Maus, J. Breuer, Development of increased test conditions for close-coupled catalyst applications, SAE 962079, 1996.
[5] R.D. O'Sullivan, N.S. Will, The effect of intermittent misfire and air to fuel ratio excursions on exhaust catalyst temperature, SAE 940927, 1994.
[6] A.P. Ngy Srun, Exhaust heat exchange coefficient in a pipe of an internal combustion engine: EGR cooler and passenger compartment heating applications, SAE 2000-01-0966, 2000.
[7] K. Sherwin, The effect of fouling on the performance of finned tube heat exchanger, SAE 971806, 1997.
[8] S.H. Lee, C.S. Bae, J.I. Jeon, T.S. Han, Effect of design parameters on the performance of finned exhaust heat exchanger, SAE 2003-01-3076, 2003.
[9] M.B. Botros, B.S. Absulnour, T.E. Smith, M.C. Lai, Optimum design parameters of an automotive blower fan housing scroll, SAE 960965, 1996.
[10] J.C. Yu, T.R. Hung, F. Thibault, Performance optimization of extrusion blow molded parts using fuzzy neural-Taguchi method and genetic algorithm, in: Proceedings of the 2002 ASME Design Engineering Technical Conferences, vol. 2, 2002, pp. 133–139.
[11] Z. Win, R.P. Gakkhar, S.C. Jain, M. Bhattacharya, Noise, emissions and fuel economy investigation on a small DI diesel using Taguchi methods, SAE 2002-32-1793, 2002.
[12] J.M. Wallace, S. Wojcik, D.N. Mavris, Robust design analysis of a gas turbine component, in: Proceedings of the ASME Turbo Expo 2003, vol. 6B, 2003, pp. 1265–1272.
[13] J. Antony, M. Kaye, Experimental Quality—A Strategic Approach to Achieve and Improve Quality, Kluwer Academy Publisher, 1999.
[14] W.Y. Fowlkes, C.M. Creveling, Engineering Methods for Robust Product Design—Using Taguchi Methods in Technology and Product Development, Addison-Wesley Publishing Company, 1995.
[15] K.-L. Tsui, An overview of Taguchi method and newly developed statistical methods for robust design, IEEE Transactions 24 (5) (1992) 44–55.
[16] J. Windmann, J. Braun, P. Zacke, S. Tischer, O. Deutschmann, J. Warnatz, Impact of the inlet flow distribution on the light-off behavior of a 3-way catalytic converter, SAE 2003-03-0937, 2003.
[17] F.P. Incropera, D.P. Dewitt, Fundamentals of heat and mass transfer, fourth ed., John Wiley & Sons, 1996.
[18] G. Taguchi, Robust technology development, Mech. Engrg. 115 (3) (1993) 60–62.
[19] G. Taguchi, S.C. Tsai, Quality engineering (Taguchi method) for the development of electric circuit technology, IEEE Trans. 44 (2) (1995) 225–229.
[20] G. Taguchi, Taguchi methods in LSI fabrication process, in: IEEE International 6th Workshop on Statistical methodology, 2001, pp. 1–6.